Appl. Math. Mech. -Engl. Ed., **39**(10), 1425–1436 (2018)

Applied Mathematics and Mechanics (English Edition)

https://doi.org/10.1007/s10483-018-2377-7

Natural convection of an alumina-water nanofluid inside an inclined wavy-walled cavity with a non-uniform heating using Tiwari and Das' nanofluid model*

M. A. SHEREMET[1], R. TRÎMBIŢAŞ[2,†], T. GROŞAN[2], I. POP[2]

1. Laboratory on Convective Heat and Mass Transfer, Tomsk State University, Tomsk 634050, Russia;

2. Department of Mathematics, Babeş-Bolyai University, Cluj-Napoca 400084, Romania

(Received Feb. 21, 2018 / Revised May 9, 2018)

Abstract The present study is devoted to numerical analysis of natural convective heat transfer and fluid flow of alumina-water nanofluid in an inclined wavy-walled cavity under the effect of non-uniform heating. A single-phase nanofluid model with experimental correlations for the nanofluid viscosity and thermal conductivity has been included in the mathematical model. The considered governing equations formulated in dimensionless stream function, vorticity, and temperature have been solved by the finite difference method. The cavity inclination angle and irregular walls (wavy and undulation numbers) are very good control parameters for the heat transfer and fluid flow. Nowadays, optimal parameters are necessary for the heat transfer enhancement in different practical applications. The effects of the involved parameters on the streamlines and isotherms as well as on the average Nusselt number and nanofluid flow rate have been analyzed. It has been found that the heat transfer rate and fluid flow rate are non-monotonic functions of the cavity inclination angle and undulation number.

Key words wavy cavity, natural convection, Al_2O_3-water nanofluid, non-uniform heating, numerical result

Chinese Library Classification O361
2010 Mathematics Subject Classification 76S05, 80A20, 76R10, 65N06

Nomenclature

a, b,	wavy wall parameters;	k,	thermal conductivity;
c_p,	specific heat at constant pressure;	L, H,	cavity sizes (width, height);
g,	gravitational acceleration vector;	Nu,	local Nusselt number;
Gr,	Grashof number;	$\overline{Nu}$,	average Nusselt number;
H_1, H_2, H_3,	additional functions;	p,	dimensional pressure;

* Citation: SHEREMET, M. A., TRÎMBIŢAŞ, R., GROŞAN, T., and POP, I. Natural convection of an alumina-water nanofluid inside an inclined wavy-walled cavity with a non-uniform heating using Tiwari and Das' nanofluid model. *Applied Mathematics and Mechanics* (*English Edition*), **39**(10), 1425–1436 (2018) https://doi.org/10.1007/s10483-018-2377-7

† Corresponding author, E-mail: tradu@math.ubbcluj.ro

Project supported by the Ministry of Education and Science of the Russian Federation (No. 13.6542.2017/6.7)

Pr,	Prandtl number;	T_{w},	non-uniform temperature of the bottom wall;
Ra,	Rayleigh number;	u, v,	dimensionless velocity components;
T,	dimensional temperature;	$\overline{u}, \overline{v}$,	dimensional velocity components;
t,	dimensional time;	x, y,	dimensionless Cartesian coordinates;
T_{c},	cold temperature of left and right vertical walls and upper wall;	$\overline{x}, \overline{y}$,	dimensional Cartesian coordinates.

Greek symbols

α,	thermal diffusivity;	ρ,	density;
β,	thermal expansion coefficient;	ρ_{c},	heat capacitance;
γ,	cavity inclination angle;	ρ_β,	buoyancy coefficient;
θ,	dimensionless temperature;	τ,	dimensionless time;
κ,	undulation number;	ϕ,	nanoparticles volume fraction;
μ,	dynamic viscosity;	ψ,	dimensionless stream function;
ξ, η,	new independent variables;	ω,	dimensionless.

Subscripts

c,	cold;	nf,	nanofluid;
f,	fluid;	p,	particle.

1 Introduction

Natural convection is an important topic for different technologies and engineering analysis. It has wide applications in engineering such as solar applications, civil constructions, electronic industry, industrial boilers, and ovens with porous materials. The boundaries can be open or closed geometries with working fluid that can be regular fluids (Newtonian) or nanofluids. Convective heat transfer of nanofluids has been extensively studied in recent years. Conventional heat transfer fluids such as water, oil, or ethylene glycol have low thermal conductivity, which is a primary limitation in enhancing the performance and the compactness of many engineering electronic devices. Therefore, there is a need to develop advanced heat transfer fluids with substantially higher conductivities. With recently introduced nanofluids, which are the fluids with suspended solid nanoparticles of higher thermal conductivity such as metals within it, the aforementioned need has been overcome.

It seems that Choi[1] is the first author to use the term "nanofluid" in 1995, which refers to the fluid with suspended nanoparticles. It is known that heat transfer can be enhanced by employing various techniques and methodologies, such as increasing either the heat transfer surface or the heat transfer coefficient between the fluid and the surface, that allow high heat transfer rates in a small volume[2]. Cooling is one of the most important technical challenges facing many diverse industries, including microelectronics, transportation, solid-state lighting, and manufacturing. The addition of nanometer-sized solid metal or metal oxide particles to the base fluids shows an increment in the thermal conductivity of the resultant nanofluids. Nanoparticles materials may be taken as oxides (Al_2O_3, CuO), metal carbides (SiC), nitrides (AlN, SiN) or metals (Al, Cu), etc. Base fluids are water, ethylene or tri-ethylene-glycols and other coolants, oil and other lubricants, bio-fluids, polymer solutions, other common fluids. In recent years, considerable interest has been shown in the study of nanofluid, which has become an innovative idea for thermal engineering, because it has various applications in automotive industries, energy saving, nuclear reactors, developed medical applications including cancer therapy, etc. Routbort[3] who employed nanofluids for industrial cooling showed that it can result in great energy savings and emission reductions. Donzelli et al.[4] showed that a particular class of nanofluids can be used as a smart material working as a heat valve to control the flow of heat.

There are many papers published on the application of nanofluids in cavities, and several related papers were those by Khanafer et al.[5], Tiwari and Das[6], Oztop and Abu-Nada[7], Sheremet et al.[8], Ghalambaz et al.[9–10], Chamkha et al.[11], Revnic et al.[12], etc.

Wavy walled cavities can be seen in different engineering applications such as heat exchangers, solar energy applications or buildings (Heidary and Kermani[13], Wang and Zhao[14], and Yuan and Zhao[15]). In this context, Cho et al.[16] presented an application on natural convection and entropy generation in a nanofluid filled cavity. Billah et al.[17] made a numerical simulation on buoyancy-driven heat and fluid flow in a nanofluid-filled triangular enclosure as an application of curvilinear boundaries. They used the Galerkin finite element method to solve the governing equations and found that heat transfer was increased by 25% as volume fraction increases from 0% to 8% when $Gr = 10^5$. Other applications on wavy-walled enclosure filled with nanofluid can be found for wavy-walled porous cavity with a nanofluid presented by Sheremet et al.[18–20] and combined convection flow in a triangular wavy chamber by Nasrin et al.[21].

It is worth mentioning that many references on nanofluids can be found in the books by Das et al.[22], Nield and Bejan[23], and Shenoy et al.[24], and in the review papers by Buongiorno et al.[25], Kakaç and Pramuanjaroenkij[26], Wong and Leon[27], Manca et al.[2], Mahian et al.[28], Sheikholeslami and Ganji[29], Groşan et al.[30], Myers et al.[31], etc.

Motivated by these studies, the objective of the present work is to numerically study the natural convection heat transfer of nanofluids inside an inclined wavy-walled cavity with a non-uniform heating using a single-phase nanofluid model[6] with experimental-based correlations for the properties of nanofluids. A systematic study of the effects of the various pertinent parameters on flow and heat transfer characteristic is carried out with the help of graphs. To the best of the authors' knowledge, the results of the present study are new and have not been reported before.

2 Basic equations

Consider the natural convection flow and heat transfer in an inclined wavy cavity having impermeable rigid walls and filled by a water-based nanofluid with solid alumina nanoparticles. A schematic geometry of the problem under investigation is shown in Fig. 1, where the $\overline{x}$ axis is measured along the lower wall of the cavity, the $\overline{y}$ axis is measured along the vertical wall of the cavity, L is the bottom wall length, and H is the height of the vertical wall. It is assumed that the bottom wall is heated sinusoidally,

$$T_{\mathrm{w}}(\overline{x}) = T_{\mathrm{c}} + \frac{\Delta T}{2}\left(1 - \cos\left(\frac{2\pi\overline{x}}{L}\right)\right),$$

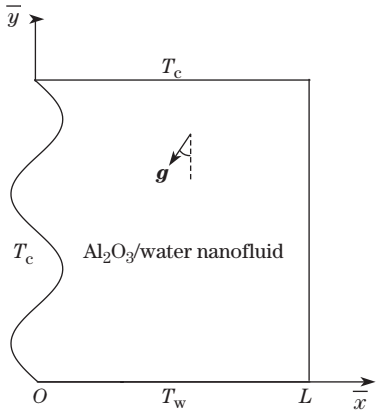

Fig. 1 Physical model and coordinate system

where ΔT is the temperature difference between the maximum and minimum temperatures, while other walls are kept at constant low temperature T_c. The thermophysical properties of the base fluid and the alumina nanoparticles are given by Oztop and Abu-Nada[7]. The left wavy wall and right flat wall of the cavity are described by $\overline{x}_1 = L - L(a + b\cos(2\pi\kappa\overline{y}/H))$ and $\overline{x}_2 = L$, respectively, and $\Delta\overline{x} = \overline{x_2} - \overline{x_1} = L(a + b\cos(2\pi\kappa\overline{y}/H))$.

Using the Boussinesq law and taking into account the above-mentioned assumptions, the governing equations can be written as follows:

$$\nabla \cdot \boldsymbol{V} = 0, \tag{1}$$

$$\rho_{\rm nf}\Big(\frac{\partial \boldsymbol{V}}{\partial t} + (\boldsymbol{V}\cdot\nabla)\boldsymbol{V}\Big) = -\nabla p + \mu_{\rm nf}\nabla^2\boldsymbol{V} - (\rho_\beta)_{\rm nf}(T - T_c)\boldsymbol{g}, \tag{2}$$

$$(\rho_c)_{\rm nf}\Big(\frac{\partial T}{\partial t} + (\boldsymbol{V}\cdot\nabla)T\Big) = k_{\rm nf}\Big(\frac{\partial^2 T}{\partial \overline{x}^2} + \frac{\partial^2 T}{\partial \overline{y}^2}\Big), \tag{3}$$

and in the Cartesian coordinates,

$$\frac{\partial \overline{u}}{\partial \overline{x}} + \frac{\partial \overline{v}}{\partial \overline{y}} = 0, \tag{4}$$

$$\rho_{\rm nf}\Big(\frac{\partial \overline{u}}{\partial t} + \overline{u}\frac{\partial \overline{u}}{\partial \overline{x}} + \overline{v}\frac{\partial \overline{u}}{\partial \overline{y}}\Big) = -\frac{\partial p}{\partial \overline{x}} + \mu_{\rm nf}\Big(\frac{\partial^2 \overline{u}}{\partial \overline{x}^2} + \frac{\partial^2 \overline{u}}{\partial \overline{y}^2}\Big) + (\rho_\beta)_{\rm nf} g(T - T_c)\sin(\gamma), \tag{5}$$

$$\rho_{\rm nf}\Big(\frac{\partial \overline{v}}{\partial t} + \overline{u}\frac{\partial \overline{v}}{\partial \overline{x}} + \overline{v}\frac{\partial \overline{v}}{\partial \overline{y}}\Big) = -\frac{\partial p}{\partial \overline{y}} + \mu_{\rm nf}\Big(\frac{\partial^2 \overline{v}}{\partial \overline{x}^2} + \frac{\partial^2 \overline{v}}{\partial \overline{y}^2}\Big) + (\rho_\beta)_{\rm nf} g(T - T_c)\cos(\gamma), \tag{6}$$

$$\frac{\partial T}{\partial t} + \overline{u}\frac{\partial T}{\partial \overline{x}} + \overline{v}\frac{\partial T}{\partial \overline{y}} = \alpha_{\rm nf}\Big(\frac{\partial^2 T}{\partial \overline{x}^2} + \frac{\partial^2 T}{\partial \overline{y}^2}\Big), \tag{7}$$

where the nanofluid parameters are[7,24,32]

$$\begin{cases} \rho_{\rm nf} = (1-\phi)\rho_{\rm f} + \phi\rho_{\rm p}, \quad (\rho_c)_{\rm nf} = (1-\phi)(\rho_c)_{\rm f} + \phi(\rho_c)_{\rm p}, \\ (\rho_\beta)_{\rm nf} = (1-\phi)(\rho_\beta)_{\rm f} + \phi(\rho_\beta)_{\rm p}, \\ k_{\rm nf} = k_{\rm f}(1 + 2.944\phi + 19.67\phi^2), \quad \mu_{\rm nf} = \mu_{\rm f}(1 + 4.93\phi + 222.4\phi^2). \end{cases} \tag{8}$$

Further, we introduce the following dimensionless variables:

$$\begin{cases} x = \overline{x}/L, \quad y = \overline{y}/L, \quad \tau = t\sqrt{g\beta\Delta T/L}, \quad u = \overline{u}/\sqrt{g\beta\Delta T L}, \\ v = \overline{v}/\sqrt{g\beta\Delta T L}, \quad \theta = (T - T_c)/\Delta T, \end{cases} \tag{9}$$

and dimensionless stream function ψ and vorticity ω

$$u = \frac{\partial \psi}{\partial y}, \quad v = -\frac{\partial \psi}{\partial x}, \quad \omega = \frac{\partial v}{\partial x} - \frac{\partial u}{\partial y}. \tag{10}$$

As a result, the governing equations (4)–(7) can be rewritten in dimensionless forms as

$$\frac{\partial^2 \psi}{\partial x^2} + \frac{\partial^2 \psi}{\partial y^2} = -\omega, \tag{11}$$

$$\frac{\partial \omega}{\partial \tau} + \frac{\partial \psi}{\partial y}\frac{\partial \omega}{\partial x} - \frac{\partial \psi}{\partial x}\frac{\partial \omega}{\partial y} = H_1(\phi)\sqrt{\frac{Pr}{Ra}}\Big(\frac{\partial^2 \omega}{\partial x^2} + \frac{\partial^2 \omega}{\partial y^2}\Big) + H_2(\phi)\Big(\frac{\partial \theta}{\partial x}\cos\gamma - \frac{\partial \theta}{\partial y}\sin\gamma\Big), \tag{12}$$

$$\frac{\partial \theta}{\partial \tau} + \frac{\partial \psi}{\partial y}\frac{\partial \theta}{\partial x} - \frac{\partial \psi}{\partial x}\frac{\partial \theta}{\partial y} = \frac{H_3(\phi)}{\sqrt{Ra\cdot Pr}}\Big(\frac{\partial^2 \theta}{\partial x^2} + \frac{\partial^2 \theta}{\partial y^2}\Big) \tag{13}$$

along with the corresponding boundary conditions

$$\begin{cases} \psi = 0, \quad \theta = 0 \quad \text{on} \quad x = x_1, \\ \psi = 0, \quad \theta = 0 \quad \text{on} \quad x = x_2, \\ \psi = 0, \quad \theta = 0.5(1 - \cos(2\pi x)) \quad \text{on} \quad y = 0, \\ \psi = 0, \quad \theta = 0 \quad \text{on} \quad y = A, \end{cases} \tag{14}$$

where $x_1 = 1 - a - b\cos(2\pi\kappa y/A)$ and $x_1 = 2$ with $\Delta x = x_2 - x_1 = a + b\cos(2\pi\kappa y/A)$ and $A = H/L$.

Here, $Pr = \frac{\mu_{\rm f}/\rho_{\rm f}}{K_{\rm f}/(\rho c_p)_{\rm f}}$ is the Prandtl number, $Ra = g(\rho_\beta)_{\rm f}\Delta T L^3/(\alpha\mu)_{\rm f}$ is the Rayleigh number, $A = H/L$ is the aspect ratio of the cavity, and the functions $H_1(\phi)$, $H_2(\phi)$, and $H_3(\phi)$ are given by

$$\begin{cases} H_1(\phi) = \dfrac{1 + 4.93\phi + 222.4\phi^2}{1 - \phi + \phi\rho_{\rm p}/\rho_{\rm f}}, \\ H_2(\phi) = \dfrac{1 - \phi + \phi(\rho_\beta)_{\rm p}/(\rho_\beta)_{\rm f}}{1 - \phi + \phi\rho_{\rm p}/\rho_{\rm f}}, \\ H_3(\phi) = \dfrac{1 + 2.944\phi + 19.67\phi^2}{1 - \phi + \phi(\rho_{\rm c})_{\rm p}/(\rho_{\rm c})_{\rm f}}. \end{cases} \tag{15}$$

It should be noted that for the present study the no-slip conditions have been used in Eq. (14) for the nanofluid velocities at the rigid walls. It is worth mentioning that the velocity boundary conditions can be more complex[33–34].

3 Numerical method and validation

The cavity in the x and y planes, i.e., physical domain, is transformed into a rectangular geometry in the computational domain using an algebraic coordinate transformation by introducing new independent variables ξ and η in the form,

$$\begin{cases} \xi = \dfrac{x - x_1}{\Delta x} = \dfrac{x - 1 + a + b\cos(2\pi\kappa y/A)}{a + b\cos(2\pi\kappa y/A)}, \\ \eta = y. \end{cases} \tag{16}$$

Using the transformation (16), the governing equations (11)–(13) can be rewritten in the following forms:

$$\Big(\Big(\frac{\partial\xi}{\partial x}\Big)^2 + \Big(\frac{\partial\xi}{\partial y}\Big)^2\Big)\frac{\partial^2\psi}{\partial\xi^2} + 2\frac{\partial\xi}{\partial y}\,\frac{\partial^2\psi}{\partial\xi\partial\eta} + \frac{\partial^2\psi}{\partial\eta^2} + \frac{\partial^2\xi}{\partial y^2}\,\frac{\partial\psi}{\partial\xi} = -\omega, \tag{17}$$

$$\begin{aligned} &\frac{\partial\omega}{\partial\tau} + \frac{\partial\xi}{\partial x}\,\frac{\partial\psi}{\partial\eta}\,\frac{\partial\omega}{\partial\xi} - \frac{\partial\xi}{\partial x}\,\frac{\partial\psi}{\partial\xi}\,\frac{\partial\omega}{\partial\eta} \\ &= H_1(\phi)\sqrt{\frac{Pr}{Ra}}\Big(\Big(\Big(\frac{\partial\xi}{\partial x}\Big)^2 + \Big(\frac{\partial\xi}{\partial y}\Big)^2\Big)\frac{\partial^2\omega}{\partial\xi^2} + 2\frac{\partial\xi}{\partial y}\,\frac{\partial^2\omega}{\partial\xi\partial\eta} + \frac{\partial^2\omega}{\partial\eta^2} + \frac{\partial^2\xi}{\partial y^2}\,\frac{\partial\omega}{\partial\xi}\Big) \\ &\quad + H_2(\phi)\Big(\frac{\partial\xi}{\partial x}\,\frac{\partial\theta}{\partial\xi}\cos\gamma - \Big(\frac{\partial\xi}{\partial y}\,\frac{\partial\theta}{\partial\xi} + \frac{\partial\theta}{\partial\eta}\Big)\sin\gamma\Big), \end{aligned} \tag{18}$$

$$\begin{aligned} &\frac{\partial\theta}{\partial\tau} + \frac{\partial\xi}{\partial x}\,\frac{\partial\psi}{\partial\eta}\,\frac{\partial\theta}{\partial\xi} - \frac{\partial\xi}{\partial x}\,\frac{\partial\psi}{\partial\xi}\,\frac{\partial\theta}{\partial\eta} \\ &= \frac{H_3(\phi)}{\sqrt{Ra\cdot Pr}}\Big(\Big(\Big(\frac{\partial\xi}{\partial x}\Big)^2 + \Big(\frac{\partial\xi}{\partial y}\Big)^2\Big)\frac{\partial^2\theta}{\partial\xi^2} + 2\frac{\partial\xi}{\partial y}\,\frac{\partial^2\theta}{\partial\xi\partial\eta} + \frac{\partial^2\theta}{\partial\eta^2} + \frac{\partial^2\xi}{\partial y^2}\,\frac{\partial\theta}{\partial\xi}\Big). \end{aligned} \tag{19}$$

The corresponding boundary conditions of these equations are given by

$$\begin{cases} \psi = 0, \quad \theta = 0 \quad \text{on} \quad \xi = 0, \\ \psi = 0, \quad \theta = 0 \quad \text{on} \quad \xi = 1, \\ \psi = 0, \quad \theta = 0.5(1 - \cos(2\pi\xi)) \quad \text{on} \quad \eta = 0, \\ \psi = 0, \quad \theta = 0 \quad \text{on} \quad \eta = A. \end{cases} \tag{20}$$

It should be noted here that

$$\frac{\partial \xi}{\partial x} = \frac{1}{a + b\cos(2\pi\kappa y/A)}, \quad \frac{\partial \xi}{\partial y} = \frac{2\pi\kappa b(x-1)\sin(2\pi\kappa y/A)}{A(a + b\cos(2\pi\kappa y/A))^2}, \quad \frac{\partial^2 \xi}{\partial x^2} = 0,$$

$$\frac{\partial^2 \xi}{\partial y^2} = \frac{4\pi^2\kappa^2(x-1)(a\cos(2\pi\kappa y/A) + b + b\sin^2(2\pi\kappa y/A))}{A^2(a + b\cos(2\pi\kappa y/A))^3}.$$

The physical quantities of interest are the local and average Nusselt numbers at the bottom wall,

$$Nu = -\frac{k_{\text{nf}}}{k_{\text{f}}} \frac{\partial \theta}{\partial \eta}, \quad \overline{Nu} = \int_0^1 Nu \, \mathrm{d}\xi. \tag{21}$$

The partial differential equations (17)–(19) with the corresponding boundary conditions (20) are solved using the finite difference method of the second order accuracy. Detailed description of the used numerical technique with comprehensive verification can be found in Refs. [8, 18–20, 24]. The grid independent solution is performed by preparing the solution for natural convection in an inclined wavy cavity filled with an alumina-water nanofluid at $Ra = 10^5$, $Pr = 6.82$, $\gamma = \pi/4$, $\phi = 0.02$, $\kappa = 2$, $a = 0.9$, $b = 0.1$, and $A = 1$. Four cases of the uniform grid are tested: a grid of 100×100 points, a grid of 150×150 points, a grid of 200×200 points, and a much finer grid of 300×300 points. Figure 2 shows an effect of the mesh parameters on the average Nusselt number and nanofluid flow rate inside the cavity.

On the basis of the conducted verifications, the uniform grid of 150×150 points has been selected for the following analysis.

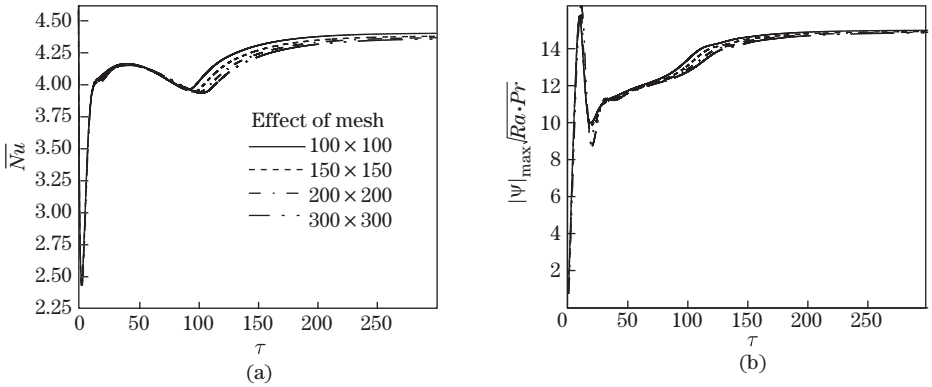

Fig. 2 Variation of the average Nusselt number (a) and nanofluid flow rate (b) versus the dimensionless time and the mesh parameters

4 Results and discussion

Numerical study has been performed at the following values of the governing parameters: Rayleigh number ($Ra = 10^5$), Prandtl number ($Pr = 6.82$), cavity inclination angle ($\gamma =$

$0.0 - \pi/2$), nanoparticles volume fraction ($\phi = 0.0 - 0.04$), aspect ratio parameter ($A = 1$), undulation number ($\kappa = 0 - 3$), wavy contraction ratio ($b = 0.1$). Particular efforts have been focused on the effects of the cavity inclination angle, undulation number and nanoparticles volume fraction on the fluid flow and heat transfer. Streamlines and isotherms as well as average and local Nusselt numbers and nanofluid flow rate for different values of control parameters mentioned above are illustrated in Figs. 3–7.

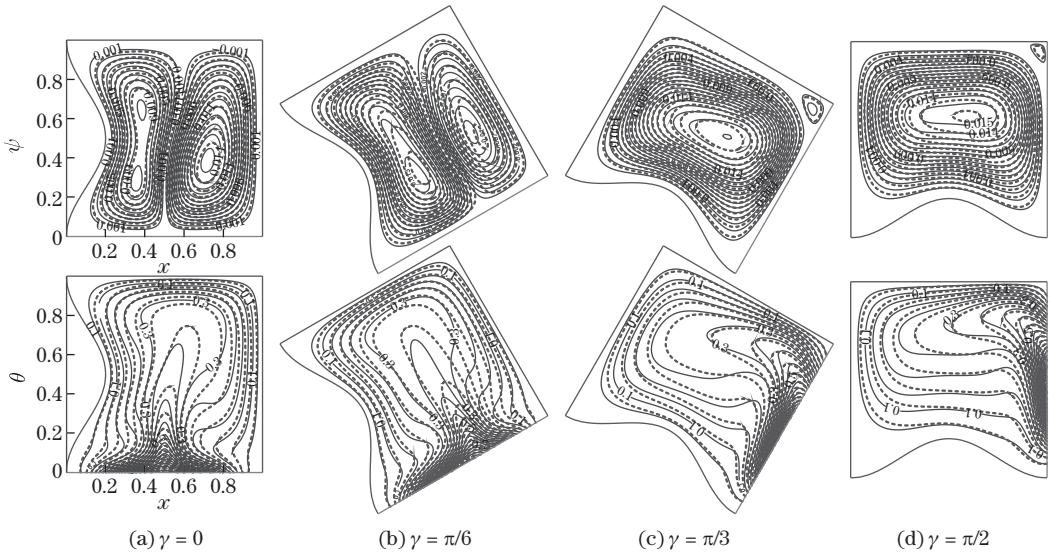

Fig. 3 Streamlines ψ and isotherms θ for $\phi = 0$ (solid lines) and $\phi = 0.04$ (dashed lines) when $\kappa = 1$

Figure 3 illustrates streamlines and isotherms inside the cavity for $\kappa = 1$ and different values of the cavity inclination angle where solid lines correspond to clear fluid ($\phi = 0$) and dashed lines correspond to nanofluid with $\phi = 0.04$. In the case $\gamma = 0$ (Fig. 3(a)), one can find a formation of two convective cells of different rotation (clockwise vortex is located near the left wall, and counterclockwise vortex is located near the wavy wall). An appearance of these circulations can be explained by a development of thermal plume over the heated wall. Taking into account the thermal boundary condition along the bottom wall ($\theta = 0.5(1 - \cos(2\pi x))$) maximum temperature $\theta = 1$ forms at $x = 0.5$. At the same time, a presence of the left wavy wall leads to weak deformation of the left circulation, where one convective cell core breaks up into two cores. Distortion of the thermal plume is also explained by the effect of wavy wall. In the case of $\gamma = \pi/6$ (Fig. 3(b)) the intensity of the left counterclockwise vortex increases and the size of this convective cell rises as well. Thermal plume weakly displaces along the heated wall due to the effect of the inclination angle and as a result of the buoyancy force influence. For $\gamma = \pi/3$ (Fig. 3(c)) and $\gamma = \pi/2$ (Fig. 3(d)), counterclockwise vortex is a major circulation with one convective cell core which is located near the heated wall. Thermal plume reflects a formation of ascending flows near the hot wall and descending one near the opposite cold wall. It should be noted that for $\gamma = \pi/2$ isotherms inside the cavity illustrate a formation of stratified temperature core with a heat conduction in the central part. It is worth noting that a dissipation of clockwise circulation occurs slowly, namely, for $\gamma = \pi/6$ (Fig. 3(b)) one can find a clockwise circulation that is commensurate to the major vortex, for $\gamma = \pi/4$ (Fig. 6(b)) the size of this minor circulation decreases, and for $\gamma = \pi/3$ (Fig. 6(c)) this circulation is vanished almost. Such effect can be explained by the influence of the buoyancy force, namely, near the heated wall under the effect of buoyancy force the hot medium ascends. Therefore, $\gamma = \pi/3$ for the cavity can be considered as a critical inclination angle when projection of the gravity

force on this wall becomes essential for the formation of ascending flow along this heated wall in comparison with projection of the gravity force on the cooled wall $x = 1$, where fluid flow begins to ascend along the cooled wall. Significant differences between clear fluid ($\phi = 0$) and nanofluid with alumina nanoparticles of $\phi = 0.04$ can be found in temperature distributions for $\gamma = 0$ and $\gamma = \pi/6$ where we have the Rayleigh-Benard convection. For $\gamma \geqslant \pi/3$ these differences are not so essential.

More detailed description of flow structures and temperature behavior with the cavity inclination angle and nanoparticles volume fraction can be found by analyzing the profiles of vertical velocity and temperature at the middle cross-section $y = 0.5$ presented in Fig. 4. In the case of the vertical velocity (Fig. 4(a)), it is possible to conclude that a growth of the inclination angle leads to a reduction of maximum vertical velocity and this maximum displaces to the wall $x = 1$. At the same time, for $\gamma = 0$ and $\gamma = \pi/6$, we have two descending flows near the walls and one ascending flow in the central part. While for $\gamma \geqslant \pi/3$, one can find a formation of one ascending flow near the wall $x = 1$ and one descending flow near the wavy wall. An addition of nanoparticles leads to a reduction of the vertical velocity for ascending and descending flows. In the case of temperature profiles, the behavior is the same, namely, a growth of the cavity inclination angle leads to both a diminution of the maximum temperature and a displacement of this maximum up to the wall $x = 1$. It is worth noting that an insertion of alumina nanoparticles illustrates a growth of temperature that is more significant for $\gamma \leqslant \pi/6$ in the central part of the cavity, while near the walls we have the opposite behavior.

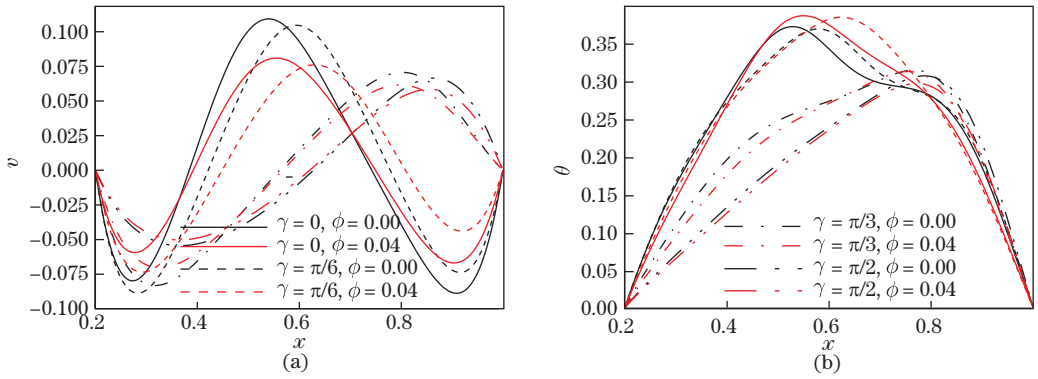

Fig. 4 Profiles vertical velocity (a) and temperature (b) at middle cross-section $y = 0.5$ for $\kappa = 1$ and different values of cavity inclination angle and nanoparticle volume fraction (color online)

Profiles of local Nusselt number for $\kappa = 1$ and different values of cavity inclination angle and nanoparticles volume fraction are demonstrated in Fig. 5. For $\gamma = 0$ one can find two local maxima and one local minimum with global minima near the walls. Such behavior can be explained by a presence of maximum temperature at $x = 0.5$, where temperature gradient decreases, while two maxima reflect a development of thermal plume. In the case of $\gamma = \pi/6$ due to a displacement of thermal plume one can find a formation of one global maximum and one local maximum. The maximum value of the local Nusselt number is due to high value of the temperature gradient in this zone. For $\gamma = \pi/3$ and $\gamma = \pi/2$, we have negative values of local Nusselt number that characterizes a heating from the medium to the wall due to variable temperature along the heated wall and prostrate shape of the thermal plume.

Figure 6 shows streamlines and isotherms for $\gamma = \pi/4$ and different values of the undulation number. A growth of the undulation number deforms the convective cells inside the cavity with the temperature distributions. It should be noted that various values of the undulation number reflect various deformation points inside the fluid circulation zone, namely, the major convective cell core tends to place in front of the wavy trough and it displaces in direction to

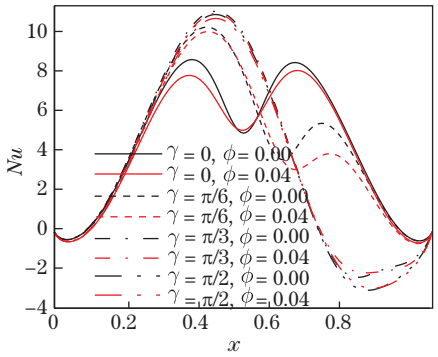

Fig. 5 Profiles of local Nusselt number along heating wall at $\kappa = 1$ for different values of cavity inclination angle and nanoparticle volume fraction (color online)

the heated wall. At the same time, an insertion of wavy wall results in a widening of the minor convective cell placed near the straight wall. An addition of nanoparticles essentially changes the flow structures, namely, the clockwise vortex dissipates due to circulation of more viscous medium.

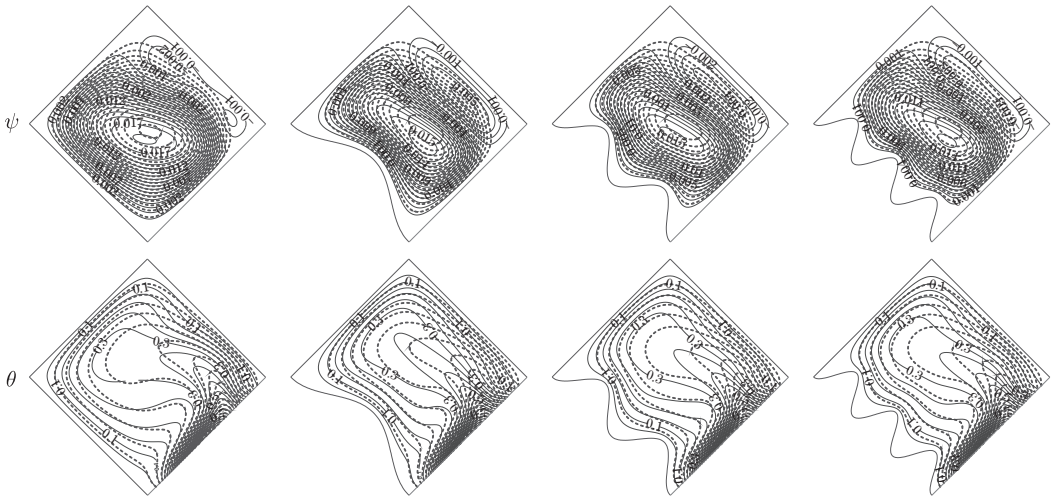

(a) $\kappa = 0$ (b) $\kappa = 1$ (c) $\kappa = 2$ (d) $\kappa = 3$

Fig. 6 Streamlines ψ and isotherms θ for $\phi = 0$ (solid lines) and $\phi = 0.04$ (dashed lines) when $\gamma = \pi/4$

Variations of the average Nusselt number and fluid flow rate for different values of the cavity inclination angle, undulation number and nanoparticles volume fraction are presented in Fig. 7. Taking into account these results, we can conclude that for $\gamma \in (0, \pi/2)$ we have low and high values of the heat transfer rate. The heat transfer reduction has been obtained for $\gamma = \pi/4$ in the case of clear fluid and for $\gamma = \pi/6$ in the case of nanofluid with $\phi = 0.04$. Such behavior can be explained by interaction between the thermal plumes from the heated wall and wavy wall. At the same time fluid flow rate has also a non-monotonic behavior with γ.

A growth of the undulation number characterizes the heat transfer rate reduction for $0 \leqslant \kappa \leqslant 2$, while for $\kappa = 3$ the average Nusselt number increases in comparison with the case of $\kappa = 2$. Behavior of the fluid flow rate is similar to $\overline{Nu}$ with κ. An addition of nanoparticles illustrates a displacement of minimum value for the heat transfer rate and fluid flow rate at the inclination angle.

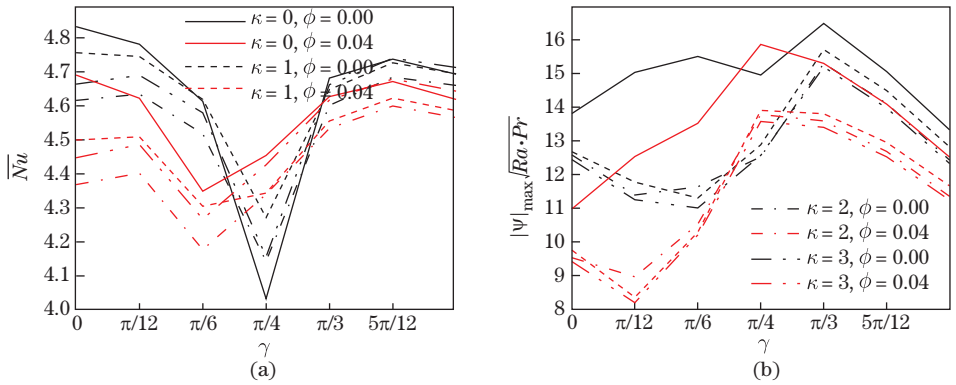

Fig. 7 Variations of average Nusselt number at heated wall (a) and nanofluid flow rate (b) with cavity inclination angle, undulation number and nanoparticle volume fraction (color online)

5 Conclusions

Natural convection of an alumina-water nanofluid within a differentially-heated wavy-walled square cavity under the effect of non-uniform heating has been numerically studied. The dimensionless governing partial differential equations have been solved numerically by using a finite difference method of the second order accuracy. The effects of the various pertinent parameters on flow and heat transfer characteristics have been graphically presented. It has been found that the cavity inclination angle, the undulation number, and the nanoparticles volume fraction are very good control parameters that can enhance the heat transfer. The average Nusselt number decreases with nanoparticles volume fraction for all values of the inclination angle, besides $\gamma = \pi/4$ where an essential heat transfer enhances with ϕ due to an addition of nanoparticles. Similar changes can be found for the fluid flow rate. An increase of the undulation number between 0 and 2 characterizes the heat transfer rate reduction, while for $\kappa \in (2, 3)$ one can find a rise of the average Nusselt number.

Acknowledgements The work of Pop, Groşan, and Trîmbiţaş has been supported from the grant PN-III-P4-ID-PCE-2016-0036, UEFISCDI, Romania. The authors also wish to express their thank to the very competent Reviewers for the valuable comments and suggestions.

References

[1] CHOI, S. U. S. Enhancing thermal conductivity of fluids with nanoparticles. *Proceedings of the* 1995 *ASME International Mechanical Engineering Congress and Exposition*, **66**, 99–105 (1995)

[2] MANCA, O., JALURIA,Y., and POULIKAKOS, D. Heat transfer in nanofluids. *Advances Mechanical Engineering*, **2010**, 380826 (2010)

[3] ROUTBORT, J. Nanofluids for Industrial Cooling Applications. *Argonne National Laboratory*, Michellin North America, Saint Gobain Corporation, Lemont (2009)

[4] DONZELLI, G., CERBINO, R., and VAILATI, A. Bistable heat transfer in a nanofluid. *Physical Letter*, **102**, 104503 (2009)

[5] KHANAFER, K., VAFAI, K., and LIGHTSTONE, M. Buoyancy-driven heat transfer enhancement in a two-dimensional enclosure utilizing nanofluids. *International Journal of Heat and Mass Transfer*, **46**, 3639–3653 (2003)

[6] TIWARI, R. J. and DAS, M. K. Heat transfer augmentation in a two-sided lid-driven differentially heated square cavity utilizing nanofluids. *International Journal of Heat and Mass Transfer*, **50**, 2002–2018 (2007)

[7] OZTOP, H. F. and ABU-NADA, E. Numerical study of natural convection in partially heated rectangular enclosures filled with nanofluids. *International Journal of Heat and Fluid Flow*, **29**, 1326–1336 (2008)

[8] SHEREMET, M. A., GROŞAN, T., and POP, I. Free convection in a square cavity filled with a porous medium saturated by nanofluid using Tiwari and Das' nanofluid model. *Transport in Porous Media*, **106**, 595–610 (2015)

[9] GHALAMBAZ, M., NOGHREHABADI, A., and GHANBARZADEH, A. Natural convection of nanofluids over a convectively heated vertical plate embedded in a porous medium. *Brazilian Journal of Chemical Engineering*, **31**, 413–427 (2014)

[10] GHALAMBAZ, M., DOOSTANI, A., IZADPANAHI, E., and CHAMKHA, A. J. Phase-change heat transfer in a cavity heated from below: the effect of utilizing single or hybrid nanoparticles as additives. *Journal of Taiwan Institute of Chemical Engineers*, **72**, 104–115 (2017)

[11] CHAMKHA, A. J., DOOSTANIDEZFULI, A., IZADPANAHI, E., and GHALAMBAZ, M. Phase-change heat transfer of single/hybrid nanoparticles-enhanced phase-change materials over a heated horizontal cylinder confined in a square cavity. *Advanced Powder Technology*, **28**, 385–397 (2017)

[12] REVNIC, C., ABU-NADA, E., GROŞAN, T., and POP, I. Natural convection in a rectangular cavity filled with nanofluids: effect of variable viscosity. *International Journal of Numerical Methods for Heat & Fluid Flow* (2018) https://doi.org/10.1108/HFF-06-2017-0244

[13] HEIDARY, H. and KERMANI, M. J. Effect of nanoparticles on forced convection in sinusoidal-wall Channel. *International Communication in Heat and Mass Transfer*, **37**, 1520–1527 (2010)

[14] WANG, Z. L. and ZHAO, Y. P. Wetting and electrowetting on corrugated substrates. *Physics of Fluids*, **29**, 067101 (2017)

[15] YUAN, Q. and ZHAO, Y. P. Multiscale dynamic wetting of a droplet on a lyophilic pillar-arrayed surface. *Journal of Fluid Mechanics*, **716**, 171–188 (2013)

[16] CHO, C. C., CHEN, C. L., and CHEN, C. K. Natural convection heat transfer and entropy generation in wavy-wall enclosure containing water-based nanofluid. *International Journal of Heat and Mass Transfer*, **61**, 749–758 (2013).

[17] BILLAH, M. M., RAHMAN, M. M., SHARIF, U. M., and ISLAM, M. N. Numerical simulation on buoyancy-driven heat transfer enhancement of nanofluids in an inclined triangular enclosure. *Procedia Engineering*, **90**, 517–523 (2014)

[18] SHEREMET, M. A., POP, I., and BACHOK, N. Effect of thermal dispersion on transient natural convection in a wavy-walled porous cavity filled with a nanofluid: Tiwari and Das' nanofluid model. *International Journal of Heat and Mass Transfer*, **92**, 1053–1060 (2016)

[19] SHEREMET, M. A., POP, I., and SHENOY, A. Natural convection in a wavy open porous cavity filled with a nanofluid: Tiwari and Das' nanofluid model. *European Physics Journal Plus*, **131**, 1–12 (2016)

[20] SHEREMET, M. A., OZTOP, H. F., POP, I., and AL-SALEM, K. MHD free convection in a wavy open porous tall cavity filled with nanofluids under an effect of corner heater. *International Journal of Heat and Mass Transfer*, **103**, 955–964 (2016)

[21] NASRIN, R., ALIM, M. A., and CHAMKHA, A. J. Combined convection flow in triangular wavy chamber filled with water-CuO nanofluid: effect of viscosity models. *International Communication in Heat and Mass Transfer*, **39**, 1226–1236 (2012)

[22] DAS, S. K., CHOI, S. U. S., YU, W., and PRADEEP, Y. *Nanofluids*: *Science and Technology*, Wiley, New Jersey (2008)

[23] NIELD, D. A. and BEJAN, A. *Convection in Porous Media*, Springer, New York (2013)

[24] SHENOY, A., SHEREMET, M., and POP, I. *Convective Flow and Heat Transfer from Wavy Surfaces*: *Viscous Fluids*, *Porous Media and Nanofluids*, CRC Press, Taylor & Francis Group, Boca Raton, New York (2016)

[25] BUONGIORNO, J. et al. A benchmark study on the thermal conductivity of nanofluids. *Journal of Applied Physics*, **106**, 1–14 (2009)

[26] KAKAÇ, S., and PRAMUANJAROENKIJ, A. Review of convective heat transfer enhancement with nanofluids. *International Journal of Heat and Mass Transfer*, **52**, 3187–3196 (2009)

[27] WONG, K. F. V. and LEON, O. D. Applications of nanofluids: current and future. *Advanced Mechanical Engineering*, **2010**, 1–11 (2010)

[28] MAHIAN, O., KIANIFAR, A., KALOGIROU, S. A., POP, I., and WONGWISES, S. A review of the applications of nanofluids in solar energy. *International Journal of Heat and Mass Transfer*, **57**, 582–594 (2013)

[29] SHEIKHOLESLAMI, M. and GANJI, D. D. Nanofluid convective heat transfer using semi analytical and numerical approaches: a review. *Journal of Taiwan Institute of Chemical Engineering*, **65**, 43–77 (2016)

[30] GROŞAN, T., SHEREMET, M. A., and POP, I. Heat transfer enhancement in cavities filled with nanofluids. *Advances in Heat Transfer Fluids*: *from Numerical to Experimental Techniques*, CRC Press, Taylor & Francis, New York, 267–284 (2017)

[31] MYERS, T. G., RIBERA, H., and CREGAN, V. Does mathematics contribute to the nanofluid debate? *International Journal of Heat and Mass Transfer*, **111**, 279–288 (2017)

[32] HO, C. J., LI, W. K., CHANG, Y. S., and LIN, C. C. Natural convection heat transfer of alumina-water nanofluid in vertical square enclosures: an experimental study. *International Journal of Thermal Science*, **49**, 1345–1353 (2010)

[33] QIN, X. Q., YUAN, Y., ZHAO, S. X., and LIU, Z. Measurement of the rate of water translocation through carbon nanotubes. *Nano Letters*, **11**, 2173–2177 (2011)

[34] YUAN, Q. Z., YANG, J. H., SUI, Y., and ZHAO, Y. P. Dynamics of dissolutive wetting: a molecular dynamics study. *Langmuir*, **33**, 6464–6470 (2017)